The 22nd Conference of Mechanical Engineering Network of Thailand
15-17 October 2008, Thammasat University, Rangsit Campus, Pathum Thani, Thailand

Embedded Force Control for a Hybrid 5-Axis H-4 Family Parallel Manipulator

Viboon Sangveraphunsiri* and Kummun Chooprasird
Robotics and Manufacturing Lab.
Department of Mechanical Engineering,Faculty of Engineering, Chulalongkorn University
Bangkok 10330, Thailand.
*E-mail: viboon.s@eng.chula.ac.th

Abstract

This paper presents the derived dynamics equations in 5 axis H-4 parallel manipulator for real-time controls using Inverse Dynamics Control for position control and Impedance Control for indirect force control strategy. Friction models obtained from the experiment are also used to compensate the actual friction of the control system. From the experimental results of the real-time control, the motion tracking and impedance force control performance are satisfaction. Tracking errors can be reduced within 0.40 millimeter by using friction compensated model. The derived dynamic model is also suitable for others advanced control technique. The accuracy of the control can be improved by increasing the rigidity of the structure.

Keywords: H-4 Parallel Robot, Resolve acceleration, Impedance Control

1. Introduction

Robot force control has attracted a wide number of researchers in the past two decades. Robots using force feedback are expected to operate in unstructured environments other than the industrial shop floor.

Control of the interaction between manipulator and the environment is crucial. Robot end effector has to perform some operation on a surface such as polishing, deburring , machining, or assembly. During interaction, the constraints which have to be set by geometric paths can be followed by the end effector. In such a case, the use of an only motion control strategy for controlling interaction is not enough. In task, due to motion errors, the manipulator may try to violate the constraints imposed by the environment. This builds to rise a contact force and a deviation of the end effector from the desired path. A compliant behavior is introduced during interaction to overcome this task.

Interaction control strategies have two categories: indirect force control and direct force control. Indirect force control is belong to compliance control and impedance control, where position error is related to contact force through a impedance with adjustable parameters.

In most situations, a model of the environment is not available. The effective strategy is the motion and force control obtained by closing a force control loop around a motion control loop.

Many advantages of the parallel mechanism robots over serial mechanism, such as structural stiffness, load capacity, accurate precision, speed and acceleration performance, induce the parallel manipulator to the topics of research activities in the academic community for several years since the 6-DOF parallel mechanism for flight simulator proposed by Gough and Stewart. Although the disabilities due to the parallel configurations are the small working volume and small movement for orientation to reach a workpiece, the benefits of these mechanisms have still been taking in development continuously in fields of robotic.

The minimum requirement to give maximum flexibility in between tool and workpiece orientation is five degrees of freedom. Besides the advantages mentioned above, the motion characteristics are also preferable such as the errors in the arms are averaged instead of build up as in series structure, the load is distributed to all arms, low inertia due to actuators are mount on a fixed base. The purposed configuration is for a rapid prototype application in the form of a master-slave application with force control algorithms.

Owing to multiple close-chain links make the dynamic analysis of parallel manipulators more complicated than serial manipulators. To obtain the dynamic model by using Newton-Euler formulation, the equations of motion of each body need to be written which leads to a large number of equations and consumes large computation time when used in a real-time control system. Unnecessary computation of reaction forces as done in the Newton-Euler formulation are eliminated in the Lagrangian formulation. Additional coordinates along with a set of Lagrangian and some model simplification make the Lagrange formulation more efficient than Newton-Euler formulation. In this paper we use the derived dynamic model of the H-4 parallel robot by using the Lagrangian for inverse dynamics control.

The intention of this article is to use inverse dynamics for motion tracking and impedance force control with inner motion tracking loop to evaluate the dynamics of a 5-DOF manipulator based on the H-4

manipulator with one rotational table by Lagrange formulation.

2. Inverse Dynamics Control

In this section, the problem of tracking control of an operational space trajectory or a Cartesian space trajectory is presented. The circular path on a spherical surface of a workpiece is the referenced path as shown in figure 1. The dynamic model of the manipulator arm can be written in the well known format as shown in equation (1). It is nonlinear and multivariable system.

$$\boldsymbol{B}(\boldsymbol{q})\ddot{\boldsymbol{q}} + \boldsymbol{C}(\boldsymbol{q},\dot{\boldsymbol{q}})\dot{\boldsymbol{q}} + \boldsymbol{F}\dot{\boldsymbol{q}} + \boldsymbol{g}(\boldsymbol{q}) = \boldsymbol{\tau} \qquad (1)$$

The resolved acceleration control is implemented base on the derived dynamic model. It is a feedback linearization control technique for tracking control problem. The controlled torques can be derived of the inverse dynamic model as in equation (2). The inverse dynamic model can be obtained from the derived dynamic model by Lagrange formulation.

$$\boldsymbol{\tau} = \boldsymbol{B}(\boldsymbol{q})\boldsymbol{\nu} + \boldsymbol{C}(\boldsymbol{q},\dot{\boldsymbol{q}})\dot{\boldsymbol{q}} + \boldsymbol{F}\dot{\boldsymbol{q}} + \boldsymbol{g}(\boldsymbol{q}) \qquad (2)$$

Substitute torques from in equation (2) into equation (1), the linear model used for controller design can be described by

$$\ddot{\boldsymbol{q}} = \boldsymbol{\nu} \qquad (3)$$

where $\boldsymbol{\nu}$ can be consider as resolved acceleration in term of joint space whose expression is to be determined yet. From analytical Jacobian, velocity relationship between end-effector and joint manipulator is in the form as

$$\boldsymbol{v}_e = \boldsymbol{J}_A^{-1}(\boldsymbol{q})\dot{\boldsymbol{q}} \qquad (4)$$

And the acceleration, $\boldsymbol{a} = \dot{\boldsymbol{v}}_e = \ddot{\boldsymbol{x}}_e$, can be derived from equation (4). The resolved acceleration can be chosen as

$$\boldsymbol{\nu} = \boldsymbol{J}(\boldsymbol{q})[\boldsymbol{a} - \dot{\boldsymbol{J}}^{-1}(\boldsymbol{q},\dot{\boldsymbol{q}})\dot{\boldsymbol{q}}] \qquad (5)$$

Where $\boldsymbol{a} = \dot{\boldsymbol{v}}_e = \ddot{\boldsymbol{x}}_e$ (6)

$\boldsymbol{a}$ can be consider as resolved acceleration in term of end-effector variables and can be selected as

$$\boldsymbol{a} = \ddot{\boldsymbol{x}}_d + \boldsymbol{K}_D(\dot{\boldsymbol{x}}_d - \dot{\boldsymbol{x}}_e) + \boldsymbol{K}_P(\boldsymbol{x}_d - \boldsymbol{x}_e) \qquad (7)$$

where $\boldsymbol{x}_d, \dot{\boldsymbol{x}}_d, \ddot{\boldsymbol{x}}_d$ is the desired path trajectory, end-effector velocity, and end-effector acceleration. So, equation (7) can be turned into the homogeneous differential equation as

$$\ddot{\tilde{\boldsymbol{x}}} + \boldsymbol{K}_D\dot{\tilde{\boldsymbol{x}}} + \boldsymbol{K}_P\tilde{\boldsymbol{x}} = 0 \qquad (8)$$

where $\tilde{\boldsymbol{x}} = \boldsymbol{x}_d - \boldsymbol{x}$. Equation (8) expresses the dynamics of position error, $\tilde{\boldsymbol{x}}$, while tracking the given trajectory, $\boldsymbol{x}_d, \dot{\boldsymbol{x}}_d, \ddot{\boldsymbol{x}}_d$. The gain $\boldsymbol{K}_P, \boldsymbol{K}_D$ can be selected by specify the desired feed-rate.

The block diagram of the control system is illustrated in Figure 2. The trajectory, $\boldsymbol{x}_d, \dot{\boldsymbol{x}}_d, \ddot{\boldsymbol{x}}_d$, can be derived from the specified circular path on a spherical surface. $\boldsymbol{\alpha}_d, \dot{\boldsymbol{\alpha}}_d$ are the desired angular position and velocity, respectively, of the rotating table. So, the referenced input can be written as $\mathbf{x}_d(t) = \left[x_{wd}(t) \;\; y_{wd}(t) \;\; z_{wd}(t) \;\; \theta_d(t) \;\; \alpha_d(t)\right]^T$ and $\dot{\boldsymbol{x}}_d, \ddot{\boldsymbol{x}}_d$. The command torques can be derived from the inverse dynamic model. And the end-effector position and velocity in operational space can be derived from the inverse Jacobian .

The position and velocity gain used in equation (8) is chosen

$$\boldsymbol{K}_P = \begin{bmatrix} 8400 & 0 & 0 & 0 \\ 0 & 8000 & 0 & 0 \\ 0 & 0 & 8000 & 0 \\ 0 & 0 & 0 & 7000 \end{bmatrix}$$

$$\boldsymbol{K}_D = \begin{bmatrix} 90 & 0 & 0 & 0 \\ 0 & 80 & 0 & 0 \\ 0 & 0 & 80 & 0 \\ 0 & 0 & 0 & 80 \end{bmatrix}$$

Whereas the PD gain of the rotating table are

$$\boldsymbol{k}_P = 550.0 \qquad \boldsymbol{k}_D = 4.0$$

The resistant torque models due to coulomb friction are also used in the control system as feed forward to compensation the actual friction torques in the system. The modified friction torques are as following:

For motor1:

$$\tau_{friction1} = 0.0019743*\theta + 0.15$$
$$\tau_{friction2} = -0.0022429*\theta + 0.1$$

For motor2:

$$\tau_{friction1} = -0.00112815*\theta + 0.15$$
$$\tau_{friction2} = -0.00338445*\theta + 0.1$$

For motor3:

$$\tau_{friction1} = -0.0022563*\theta + 0.15$$
$$\tau_{friction2} = 0.00112815*\theta + 0.1$$

For motor4:

$$\tau_{friction1} = -0.000112815*\theta + 0.3$$
$$\tau_{friction2} = 0.00112815*\theta + 0.2$$

In this experiment, the tool-tip is desired to maintain the direction normal to the plane tangent to the spherical surface at the point of contact along the desired path. The feed rate is set equal to 27.3273 mm/sec or 1639.638 mm/min.

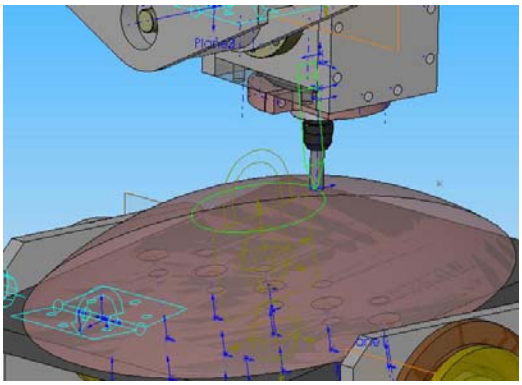

Figure 1. Circular path on spherical workpiece

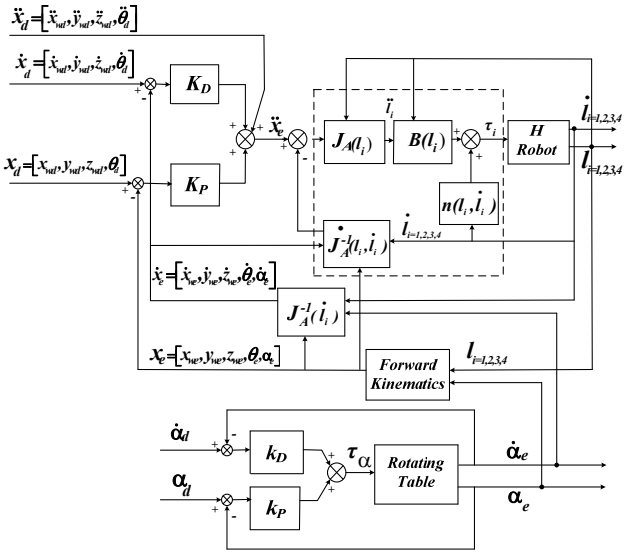

Figure 2. Block scheme of operational space inverse dynamics control

The experimental results are shown in Figure 3 – Figure 7. Figure 3 shows the measurement of the tool-tip position (Xw,Yw,Zw) in the workpiece coordinate compared with the references. Z_w is maintained in constant level at 116 mm. The actual tool-tip position is very close to the reference position. The motion in X_w and Y_w direction are sinusoidal motion. The error between the measured tool-tip position and reference position of each axis is shown in Figure 4. The maximum errors occur when the direction of motion is changed. These errors can be reduced by adding dither signal embedded in the command signal to prevent the motion get struck because of the friction. Error in both X_w and Y_w have similar pattern. The feed speed, 27.3273 mm/sec, used in this experiment is rather larger than typical cutting speed for conventional machine tool. Small backlash and structure flexibility also create sources of error. Because, in the experiment, the tool-tip position is calculated from the kinematic formulation, then the numerical truncation error also create another source of error. Figure 5 shows the tool orientation angle and angle of the rotating table which can be explained similar to the X_w and Y_w motion. The maximum error occurs in the X_w direction is less than 0.4 mm. And the maximum errors at tool-tip orientation and at the rotating table are less than 0.12 degree and 0.15 degree, respectively.

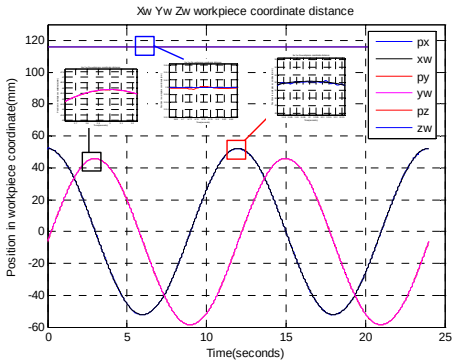

Figure 3. Tool-Tip position in workpiece coordinate Xw,Yw,Zw

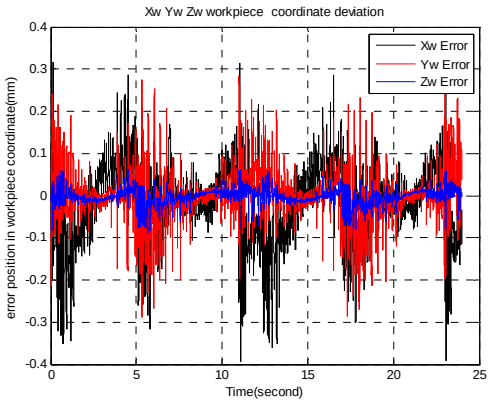

Figure 4. Tool-Tip error position in workpiece coordinate Xw,Yw,Zw

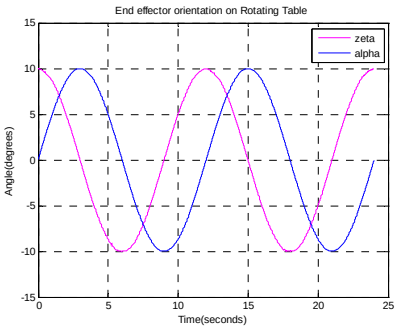

Figure 5. Tool orientation (θ) and turning table angle(α)

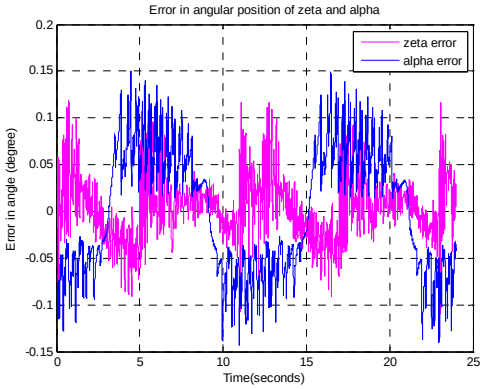

Figure 6. Tool orientation error (θ) and turning table angle error(α)

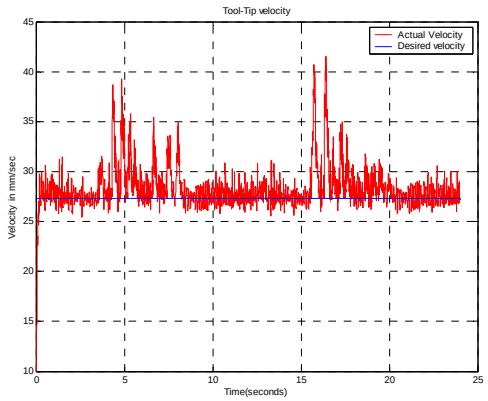

Figure 7. Tool-Tip velocity on workpiece coordinate Xw,Yw,Zw

3. Impedance Control

In this section, we focus on the problem of force control by impedance force with inner motion loop tracking. The experiment is to control the Tool-tip by tracking in the ellipse path with spherical surface obstruction as shown in figure 8. The linear impedance force control can be illustrated by:

$$M_d\Delta\ddot{p}_{dc} + D_K\Delta\dot{p}_{dc} + P_K\Delta p_{dc} = h_f \qquad (9)$$

Where M_d, D_K, P_K are positive definite and

$$h_F = \begin{bmatrix} F_X & F_Y & F_Z & M_Z \end{bmatrix}^T$$

All deviations in displacement, velocity and acceleration can be found by equation (9) as shown

$$\Delta\ddot{p}_{dc} = M_d^{-1}\left(h_F - D_K\Delta\dot{p}_{dc} - P_K\Delta p_{dc}\right) \qquad (10)$$

Where $M_d^{-1} = J_A^{-1}B^{-1}J^{-T}$ and B is the inertia matrix of H-4 manipulator from equation (1).

By chosen P_K (stiffness matrix) and D_K (damping matrix), we can solve $\Delta\ddot{p}_{dc}$. The $\Delta\dot{p}_{dc}$ and Δp_{dc} can be found by integral. Finally, the resolved acceleration can be as:

$$\ddot{x}_e = \ddot{x}_c + K_D\Delta\dot{x}_{ce} + K_P\Delta x_{ce} \qquad (11)$$

where $\ddot{x}_c = \ddot{x}_d + \Delta\ddot{p}_{dc}$

and $\Delta x_{ce} = x_c - x_e$

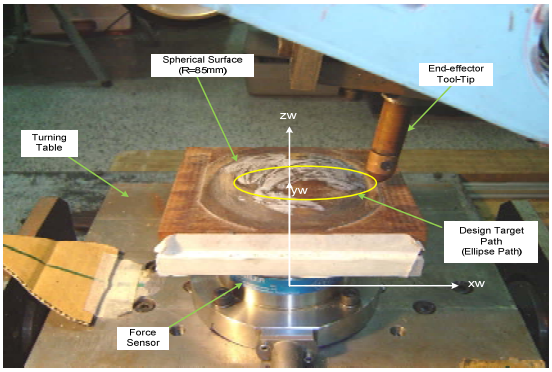

Figure 8. Ellipse path with spherical surface obstruction in Experiment

The block diagram of the Impedance control system is illustrated in Figure 9. The trajectory, $\boldsymbol{x_d}, \dot{\boldsymbol{x}}_{\boldsymbol{d}}, \ddot{\boldsymbol{x}}_{\boldsymbol{d}}$, can be derived from the specified ellipse path on a spherical surface. $\boldsymbol{\alpha_d}, \dot{\boldsymbol{\alpha}}_{\boldsymbol{d}}$ are the desired angular position and velocity, respectively, of the rotating table. So, the referenced input can be written as $\mathbf{x_d(t)} = \begin{bmatrix} x_{wd}(t) & y_{wd}(t) & z_{wd}(t) & \theta_d(t) & \alpha_d(t) \end{bmatrix}^T$ and $\dot{\boldsymbol{x}}_{\boldsymbol{d}}, \ddot{\boldsymbol{x}}_{\boldsymbol{d}}$. The deviation due to impedance force is added together with trajectory desired in order to get new desired values on compliance frame.

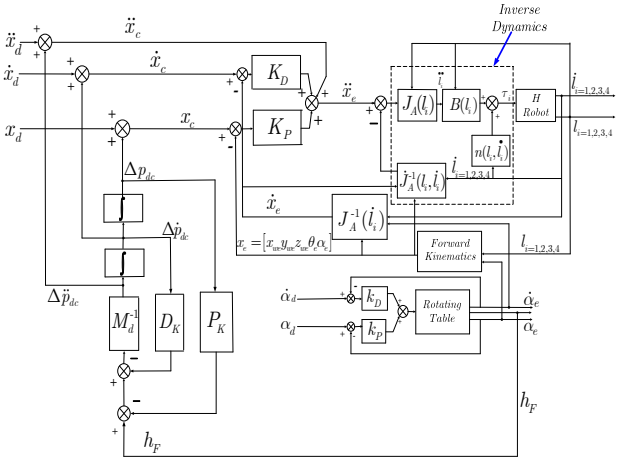

Figure 9. Block scheme of the Impedance control with Inner motion control

In this experiment, the tool-tip is desired to keep trajectory in ellipse path while as the spherical workpiece surface is an obstruction environment. Force sensor is attached on the fifth rotating axis as shown in figure 8. The stiffness matrix and damping matrix gain used in equation (10) is chosen

$$P_K = \begin{bmatrix} 6.4 & 0 & 0 & 0 \\ 0 & 8 & 0 & 0 \\ 0 & 0 & 15.42 & 0 \\ 0 & 0 & 0 & 37000 \end{bmatrix}$$

$$D_K = \begin{bmatrix} 0.7 & 0 & 0 & 0 \\ 0 & 3.6 & 0 & 0 \\ 0 & 0 & 12 & 0 \\ 0 & 0 & 0 & 9000 \end{bmatrix}$$

The gain for motion inner loop and the table is also use the same as the inverse dynamics control section.

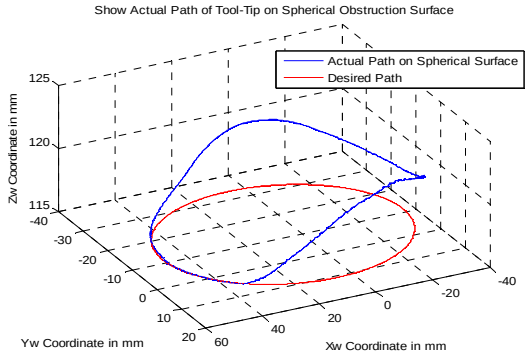

Figure10. Actual path and desired path on $X_w Y_w Z_w$

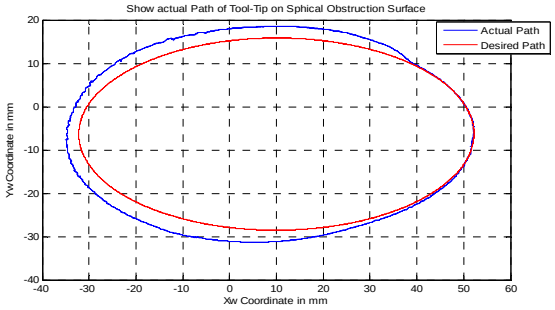

Figure11. Actual path and desired path on $X_w Y_w$ plane

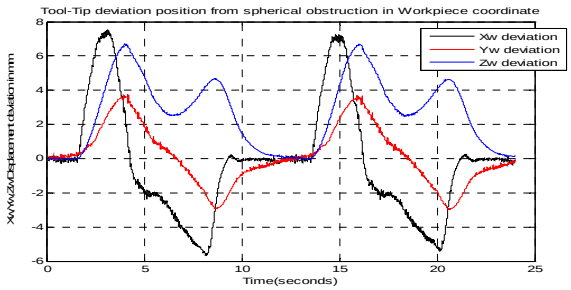

Figure12. Deviation distances on $X_w Y_w Z_w$ due to spherical obstruction.

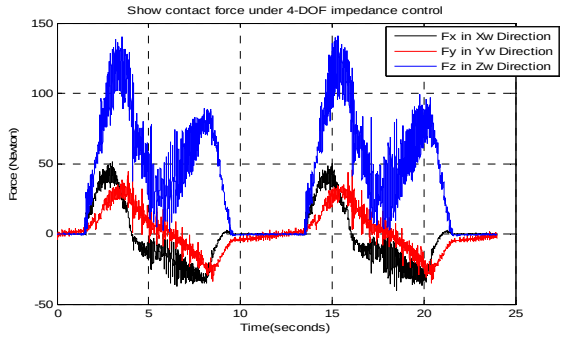

Figure13. Contact force on $X_w Y_w Z_w$ due to spherical obstruction.

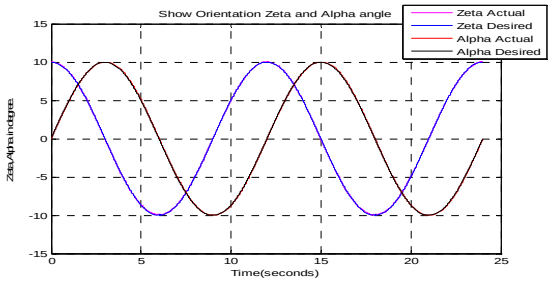

Figure14. Two Angular movement between desired and actual angular movement

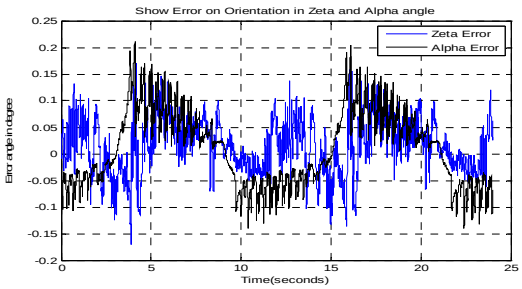

Figure15. Error in two angular movement.

The end effector moving along to the reference ellipse path has lift up and deviate from the path following the constraint spherical obstruction as in figure 10 and 11. Maximum lift is 7 mm and contact force in Z_w is 140 N. Maximum deviation in X_w is 7.5 mm and force in X_w is 50 N. Maximum deviation in Y_w is 3.5 mm and force in Y_w is 30 N as shown in figure 12 and 13.

Stiffness of the impedance system on the control strategy in along $X_w Y_w Z_w$ are as follows:

$$\frac{50}{7.5} = 6.6, \frac{30}{3.5} = 8.6, \frac{140}{7} = 20 \text{ N/m.}$$

From figure 14, the two actual angular movements follow along the desired angular movements. Error in angular movement is in 0.17 degree for θ and 0.21 degree for α as shown in figure 15.

4. Conclusion

In this paper, we presented inverse dynamics implemented in the first four axis of the H-4 parallel manipulator to perform feedback linearization. The circular trajectory on spherical surface is used as the reference profile for tracking control. The three axis impedance force control with inner motion loop strategy is introduced for real-time control to perform with spherical obstruction. The tracking performance can be improved by increasing the rigidity of the structure and reducing the numerical truncation error. The interaction performance is suitable for cooperate with master-slave operation with force feedback control.

Next, we will continue the work to cover the master-slave operation with force control algorithms for a rapid prototype manufacturing system.

References

[1]. Tsai, L. W. Robot Analysis-The Mechanics of Serial and Parallel Manipulators. John Wiley & Sons, 1999.

[2]. Bruno Siciliano, Luigi Villani. Robot Force Control. Kluwer Academic Publishers,1999.

[3]. Lorenzo Sciavicco, Bruno Siciliano. Modeling and Control of Robot Manipulators. The MacGraw-Hill Companies, Inc. 1996.

[4]. Fabrizio Caccavale, Ciro Natale, Bruno Siciliano, and Luigi Villani. Integration for the next generation Embedding Force Control into Industrial Robots. IEEE Robotics & Automation Magazine, September 2005.

[5]. Pierrot, F. H4_a new family of 4-DOF parallel robots. IEEE/ASME Advanced Intelligent Mechatronics Conf. Proc. Atlanta USA, September 1999, pp. 508-513.

[6]. Chiu, Y.J., Perng, M.H. Forward Kinematics of a General Fully Parallel Manipulator with Auxiliary Sensors. International Journal of Robotics Research vol.20 no.5, May 2001, pp. 401-414.

[7]. Pierrot, F., Marquet, F. H4 parallel robot modeling design and preliminary experiments, IEEE Robotics

and Automation Conf. Proc. Seoul Korea, May 2001, pp. 3256-3261.

[8]. Viboon S., Natdanai T., Design of the new 4-DOF parallel manipulator with object contact force control, The 19th Conference of Mechanical Engineering Network of Thailand ,October 2005.

[9]. E.L.J.Bohez , Compensating for systematic errors in 5-axis NC machining., Computer-Aided Design, 30 March 2001.

[10]. Chung-Ching Lee, Jeng-Hong Chiu Hung-Hui Wu , Kinematics of a H- Type pure Translational Parallel manipulator. Proceeding of IDETC/CIE 2005 ASME 2005 International Design Engineering Technical Conf. September 24-28,2005.

[11]. Dumitru Olaru, George C. Puiu, Liviu C. Balan, Vasile Puiu, A New Model to Estimate Friction Torque in a Ball Screw System. Product Engineering Springer Netherlands, page333-346,2005

[12]. Sangveraphunsiri,V. and Tantawiroon N., Novel Design of a 4 DOF parallel Robot., 2003 JSAE Annual Congress, Yokohama, Japan, May21-23, 2003.

[13]. Viboon Sangveraphunsiri and Tawee Ngamvilaikorn, Design and Analysis of 6 DOF Haptic Device for Teleoperation Using a Singularity-Free Parellel Mechanism, Thammasat International Journal of Science and Technology vol.10 No.4 October-December 2005,pp. 60-69.

[14]. Viboon Sangveraphunsiri and Prasartporn Wongkumchang, Design and Control of a Stewart Platform, the 15th National Conference of Mechanical Engineering,2001, (in Thai).